Hindawi
International Journal of Genomics
Volume 2019, Article ID 7350414, 13 pages
https://doi.org/10.1155/2019/7350414

Research Article

Genome-Wide Identification, Characterization, and Expression Analysis of the Grapevine Superoxide Dismutase (SOD) Family

Xiaoxuan Hu, Chenyu Hao, Zong-Ming Cheng, and Yan Zhong

College of Horticulture, Nanjing Agricultural University, Nanjing 210095, China

Correspondence should be addressed to Zong-Ming Cheng; zmc@njau.edu.cn and Yan Zhong; yzhong@njau.edu.cn

Received 5 June 2018; Revised 1 December 2018; Accepted 20 December 2018; Published 24 February 2019

Academic Editor: Giandomenico Corrado

Superoxide dismutase (SOD) is an essential enzyme of the plant antioxidant system that responds to oxidative damage caused by adverse conditions. However, little is known about the SOD gene family in *Vitis vinifera* (Vv). In the present study, ten SOD genes, including 6 copper/zinc SODs, 2 iron SODs, and 2 manganese SODs, were identified in the grapevine genome where they were unevenly distributed on 12 chromosomes. Ten VvSOD genes were divided into three main groups based on phylogenetic analysis, subcellular localization, and the distribution of conserved protein motifs. Additionally, many *cis*-elements related to different stresses were found in the promoters of the 10 VvSOD genes. Syntenic analysis revealed that *VvMSD1* and *VvMSD2* were derived from segmental duplication, and *VvCSD4* and *VvCSD5* belong to a pair of tandemly duplicated genes. Gene expression analysis based on microarray data showed that the 10 VvSOD genes were expressed in all the tested tissues. Interestingly, the segmentally duplicated gene pair (*VvMSD1* and *VvMSD2*) exhibited differential expression patterns in various organs. In contrast, the tandemly duplicated gene pair (*VvCSD4* and *VvCSD5*) displayed similar expression patterns in the tested organs. Our results provide a basis for further functional research on the SOD gene family in grapevine.

1. Introduction

Grapevine (*Vitis vinifera*) is one of the most cultivated and economically valuable fruit crops in the world. However, abiotic stresses, particularly drought and salt stress, threaten the growth of grapevine globally, thereby affecting fruit yield and quality [1–3]. The most common result of such stress is the generation of toxic reactive oxygen species (ROS). Membrane damage, protein oxidation, DNA lesions, and even irreparable metabolic dysfunction and cell death can occur as a result of excessive ROS (such as superoxide anions, hydroxyl radicals, hydrogen peroxide, and singlet oxygen) [4, 5].

To cope with ROS toxicity, plants have developed efficient and sophisticated antioxidative response systems, including the synthesis of low relative molecular mass antioxidant molecules (e.g., l-ascorbic acid and glutathione) and various enzymes. Among these enzymatic components, the superoxide dismutases (SODs) constitute the first line of defense against ROS by catalyzing the dismutation of the superoxide O_2^- to O_2 and H_2O_2 [6, 7]. In plants, SODs have been detected in the roots, leaves, fruits, and seeds where they play important roles in protecting cells from oxidative damage [8].

Multiple SOD isozymes exist in plants and are classified into three types based on their metal cofactor, protein folds, and subcellular distribution: copper/zinc- (Cu/Zn-) SOD, manganese- (Mn-) SOD, and iron- (Fe-) SOD, and these SODs are located in different compartments of the cell [7, 9, 10]. Cu/Zn-SODs are mainly distributed in the cytosol, chloroplasts, peroxisomes, and/or the extracellular space, while Fe-SODs mainly occur in the chloroplasts, as well as in peroxisomes and mitochondria, and Mn-SODs are mainly localized not only in the mitochondria but also in different types of peroxisomes [11]. In addition, a new type of SOD, nickel (Ni)SOD, was first discovered, cloned, and characterized in *Streptomyces* [12]. However, no evidence for NiSOD has been found in plants [13].

In recent years, some studies have reported that SODs contribute to the response to various environmental stimuli in plants, such as cold, drought, salinity, auxin, and ethylene [14–16]. Owing to their crucial roles in the antioxidant

system, a considerable number of SOD genes have been cloned from various monocot and dicot plants [17–19]. With the development of high-throughput sequencing technologies, the genome-wide identification of SOD gene families has been performed in many plant species, including *Arabidopsis thaliana* [20], *Dimocarpus longan* [17], *Sorghum bicolor* [21], *Populus trichocarpa* [9], *Musa acuminate* [22], *Gossypium raimondii*, *Gossypium arboreum* [23], and *Gossypium hirsutum* [24].

In the present study, we identified the SOD gene family in grapevine on the genome-wide scale. Genomic organization, gene structure, motif composition, subcellular localization, syntenic analysis, and phylogenetic relationships were analyzed using bioinformatics. Then, the gene ontology and putative promoters of the grapevine SODs were also investigated, and the *cis*-elements involved in stress responses were analyzed. Putative transcription factors (TFs) which may regulate the VvSOD genes were predicted. Furthermore, we studied the expression patterns of the grapevine SOD gene family under abiotic stress (salt, drought, cold, and heat) using microarray data and a real-time quantitative- (qRT-) PCR detection system. Finally, coexpression networks of VvSOD genes and TF genes under the four abiotic stresses were generated based on the qRT-PCR data. This was the first comprehensive study of the SOD gene family in grapevine and may provide valuable information for understanding the classification, evolution, and putative functions of the grapevine SOD family on the genome-wide scale.

2. Materials and Methods

We downloaded the most recent version (V 2.1) of a 12X assembly of the grapevine (*V. vinifera*) genome from CRIBI (http://genomes.cribi.unipd.it/grapevine/) for identifying SOD genes. To identify members of the SOD gene family in grapevine, the full-length protein sequences from *A. thaliana* (TAIR locus number: AT1G08830.1, AT2G28190, AT5G18100, AT4G25100, AT5G51100, AT5G23310, AT3G56350, and AT3G10920) were used as BLASTp queries against all the grapevine protein sequences with the threshold expectation value set to 1.0. All the hits were further submitted to Pfam analysis (http://pfam.xfam.org/) to verify the presence of the SOD domain. Physicochemical characteristics of the SOD proteins were calculated using the ProtParam tool (http://web.expasy.org/protparam/), including the number of amino acids, molecular weight, theoretical isoelectric point (pI), aliphatic index, and grand average of hydropathicity (GRAVY) [25].

ProtComp9.0 server (http://linux1.softberry.com/) was used to predict the subcellular localizations of the SOD proteins [22]. Conserved protein motifs were predicted by MEME Suite (http://meme-suite.org/tools/meme) with the default settings, except that the number of motifs was set to 8, and the minimum and maximum motif widths were set to 20 and 150 amino acids [26]. The web-based Gene Structure Display Server (GSDS; http://gsds.cbi.pku.edu.cn/index.php) program was utilized to illustrate exon and intron organization for the grapevine SOD genes.

2.1. Phylogenetic Analysis. To investigate the phylogenetic relationships of the SODs among grapevine and *A. thaliana*, multiple SOD protein sequences were aligned, and an unrooted phylogenetic tree was constructed in MEGA 6.06 [27]. The phylogenetic tree was constructed using the neighbor-joining (NJ) method and Jones-Taylor-Thornton (JTT) model. In the phylogenetic tree, the degree of support for a grouping pattern was evaluated using bootstraps (1000 replicates).

2.2. Chromosomal Locations and Syntenic Analysis. The chromosomal locations of the grapevine SOD genes were verified from the CRIBI database (http://genomes.cribi.unipd.it/grapevine/), and chromosomal images were drawn using MapInspect software [28].

Duplication patterns of the VvSOD genes were assigned based on their locations. Genes located in a 200 kb region of a chromosome or a scaffold were defined as a gene cluster derived from tandem duplications [29]. Segmentally duplicated genes were identified as genes located on duplicated chromosomal blocks and were determined using MCScanX software (http://chibba.pgml.uga.edu/mcscan2/), which detects gene duplication events using an *E*-value threshold of 10^{-5} [30].

To detect the selection mode of the segmentally duplicated gene pairs, the ratio of nonsynonymous substitutions to synonymous substitutions was evaluated. Firstly, the CDSs (nucleotide coding sequences) of the VvSOD genes were aligned using Muscle in MEGA6.06. Then, nonsynonymous substitutions (Ka), synonymous substitutions (Ks), and the ratio between them (Ka/Ks) were calculated using MEGA 6.06.

2.3. GO Analysis and Promoter Sequence Analysis. The gene ontology (GO) term IDs of each VvSOD gene member in grapevine were obtained from the CRIBI database (http://genomes.cribi.unipd.it/DATA/V2/annotation/bl2go.annot.txt). The annotations of the GO term IDs were collected from the Gene Ontology Consortium (http://www.geneontology.org). Ten grapevine SOD proteins were assessed based on their molecular functions, biological processes, and cellular localizations.

The 2000 bp upstream sequences of the coding region of each VvSOD gene were downloaded from the CRIBI database. Then, the *cis*-elements in the promoters of each VvSOD gene were predicted using the PlantCARE server (http://bioinformatics.psb.ugent.be/webtools/plantcare/html/) [31].

2.4. Prediction of Potential Regulatory Interactions between TFs and VvSODs. The TFs which possess overrepresented targets in the VvSOD gene sets were detected from the Plant Transcriptional Regulatory Map (PlantRegMap) with a regulation prediction tool (http://plantregmap.cbi.pku.edu.cn/regulation_prediction.php) [32]. 2000 bp upstream sequences of the coding region of each VvSOD gene were used as the input.

2.5. Microarray Data Analysis. Microarray gene expression profiles covering most of the grapevine organs at different stages were downloaded from Gene Expression Omnibus

(GEO, available online: https://www.ncbi.nlm.nih.gov/geo/) under the accession number GSE36128 [33]. The collected plant organs were as follows: bud, inflorescence, tendril, leaf, stem, root, developing berry, withering berry, seed, rachis, anther, carpel, petal, pollen, and seedling.

Expression analyses of SOD genes and TF genes in response to abiotic stresses were based on microarray data (including accession number GSE31594 and GSE31675) downloaded from the NCBI GEO datasets. Four abiotic stresses, including cold, salt, heat, and polyethylene glycol (PEG), were analyzed. The fold changes compared with the corresponding control in each experiment were used to generate heatmaps using the R package (https://www.r-project.org/) pheatmap.

2.6. Coexpression Network and Interaction of VvSODs and TF Genes. For the four stress treatments, the Pearson correlation coefficient (PCC) value (Table S4) was calculated between each pair of VvSODs and TF genes using gene expression values from microarray data in SPSS v 20.0 (IBM Corp., Armonk, NY, US) [28]. Coexpressed gene pairs were filtered with a PCC cutoff of 0.95. The coexpression network map was generated by Cytoscape 3.3 (http://www.cytoscape.org).

2.7. Plant Material and Experimental Treatments. For the cold, heat, and salt treatments, six-week-old "Pinot Noir" grapevine (*V. vinifera*, the sequenced genotype PN40024) plantlets were used in this study. The plantlets were maintained at a photoperiod of 16 h light/8 h dark and a temperature of 23°C. Low temperature and heat stress treatments were applied by placing the plants at 4°C (drug storage box, HYC-360, Haier) and 42°C (intelligent artificial climate box, RXZ-380C, Jiangnan Instrument Factory, Ningbo) with a photoperiod of 16 h light/8 h dark, respectively [28]. Leaf samples were harvested from both treatments at 0, 6, 12, and 24 h after initiation of the treatments. Plants subjected to 200 mmol/L NaCl were sampled at 0, 6, 12, and 24 h after treatment. Three independent biological replications were performed for each treatment. Tissue samples were immediately frozen in liquid nitrogen and stored at −70°C until analysis.

For drought stress treatment, *in vitro*-grown grapevine plants (PN40024) were maintained on half-strength Murashige and Skoog medium containing 0.3 mg/L indole 3-butyric acid (IBA) and placed at 25°C in a culture room under a photoperiod of 16/8 h and a light intensity of 100 μmol·m^{-2}·s^{-1}. Five-week-old tissue-cultured grapevine plants were transplanted into pots and acclimatized in the growth chamber with 16 h light at 24°C/8 h dark at 22°C and 70%–80% relative humidity [34]. Plants grown in pots were fully watered for the first four weeks, after which water was withheld to impose the drought treatment. The grapevine leaf samples were collected at 0 (control), 2, 4, and 8 days after the treatment, respectively.

2.8. Total RNA Extraction and cDNA Synthesis. Total RNA was extracted from the leaves using the Plant Total RNA Isolation Kit Plus. The total RNA was eluted in 30 μL of RNase-free water and stored at −70°C. The purity and density of the extracted RNA was assessed on a NanoDrop ND-1000 spectrophotometer (NanoDrop Technologies, USA) using RNase-free water as a blank.

Single-stranded cDNA was synthetized using a Takara PrimeScript RT reagent kit with a gDNA eraser (Takara, Dalian, China) and oligo dT primers as described by the manufacturer's protocol. Approximately 2 μg of total RNA in a single 20 μL reaction was converted to single-stranded cDNA using standard thermal cycling conditions.

2.9. qRT-PCR Analysis of VvSOD Genes. qRT-PCR analyses were conducted on a Roche LightCycler 480 PCR system using Lightcycler 480 SYBR Green I Master. The oligonucleotide primers (Table S3) for amplifying specific VvSODs were designed using the PrimerQuest Tool (http://sg.idtdna.com/Primerquest/Home/Index). The 10 μL reaction volume contained 5 μL SYBR Green I Master, 1 μL of diluted cDNA, 1 μL of each primer (10 μM), and the addition of ddH_2O to bring the total volume to 10 μL. The thermocycle protocol was as follows: denaturation at 95°C for 10 min, followed by 40 cycles of 95°C for 10 s, 58°C for 20 s, and 72°C for 10 s. At the end, a melting curve was generated from 65 to 97°C. Three replicates were used for each sample. Expression levels were calculated using the $2^{-\Delta\Delta T}$ method and the housekeeping gene (actin-101-like, *VIT_012s0178g00200*) was used as a reference gene for normalizing the expression of the VvSOD genes [35]. Fold differences were visualized by normalizing all of the data based on setting the expression level at 0 h as a value of 1 (values above 1 and below 1 were considered as up- and downregulated, respectively) [36].

3. Results

3.1. Genome-Wide Identification of the SOD Gene Family in Grapevine. Based on a BLAST search using the known *A. thaliana* SOD protein sequences and the identification by the Pfam database, a total of 10 SOD genes were identified in the grapevine genome. Based on the domain analysis, the 10 grapevine SOD genes were classified into 3 groups (Cu/ZnSODs, FeSODs, and MnSODs), including 6 VvSOD proteins with a copper-zinc domain (Pfam: 00080) and 4 SOD proteins with an iron/manganese superoxide dismutase alpha-hairpin domain (Pfam: 00081) or an iron/manganese superoxide dismutase, C-terminal domain (Pfam: 02777). Based on the domain analysis and chromosome location, the 10 grapevine genes were named as follows: *VvCSD1*, *VvCSD2*, *VvCSD3*, *VvCSD4*, *VvCSD5*, *VvCSD6*, *VvMSD1*, *VvMSD2*, *VvFSD1*, and *VvFSD2* (Table 1).

The physicochemical analysis indicated that the length of the amino acid sequences, MWs, pIs, aliphatic indexes, and GRAVY values varied among these VvSOD proteins. Considerable variations in the number of amino acids among these VvSOD proteins were observed, ranging from 79 to 329 aa. The predicted molecular weight of the 10 VvSOD proteins varied from 8594.7 to 37779.23 Da. The results revealed that four Fe-MnSODs were basic and five Cu/Zn-SODs were acidic, except for the slightly basic VvCSD3. The GRAVY numeric values of the three VvSOD proteins

Table 1: Chromosome location, subcellular prediction, and physicochemical properties of grape SOD proteins.

Gene name	Gene ID	ORF length	Chromosomal localization	Molecular weight	Theoretical pI	Aliphatic index	Grand average of hydropathicity (GRAVY)	Subcellular prediction
VvCSD1	VIT_202s0025g04830.1	969	chr2(4357308 4364558)	33844.25	5.66	88.66	0.007	Cytoplasmic
VvCSD2	VIT_206s0061g00750.1	666	chr6(18276905 18281206)	22537.5	5.87	92.22	0.067	Cytoplasmic
VvCSD3	VIT_208s0007g07280.1	471	chr8(20888649 20892112)	15786.74	7.19	83.78	-0.164	Cytoplasmic
VvCSD4	VIT_214s0030g00830.1	381	chr14(5076284 5079112)	12926.4	5.33	81.19	-0.202	Cytoplasmic
VvCSD5	VIT_214s0030g00950.1	351	chr14(5248285 5250067)	12149.69	4.93	84.83	0.157	Cytoplasmic
VvCSD6	VIT_214s0036g01320.1	240	chr14(12383065 12384913)	8594.7	5.81	83.67	-0.394	Cytoplasmic
VvMSD1	VIT_206s0004g07950.1	687	chr6(8686646 8687855)	25615.29	7.14	94.56	-0.358	Mitochondrial
VvMSD2	VIT_213s0067g02990.1	852	chr13(1602822 1606910)	31456.18	9.29	86.08	-0.364	Mitochondrial
VvFSD1	VIT_210s0042g00100.1	990	chr10(12756538 12763591)	37779.23	8.62	77.11	-0.522	Chloroplast
VvFSD2	VIT_216s0013g00260.1	681	chr16(5200339 5206132)	25268.79	8.48	83.76	-0.375	Chloroplast

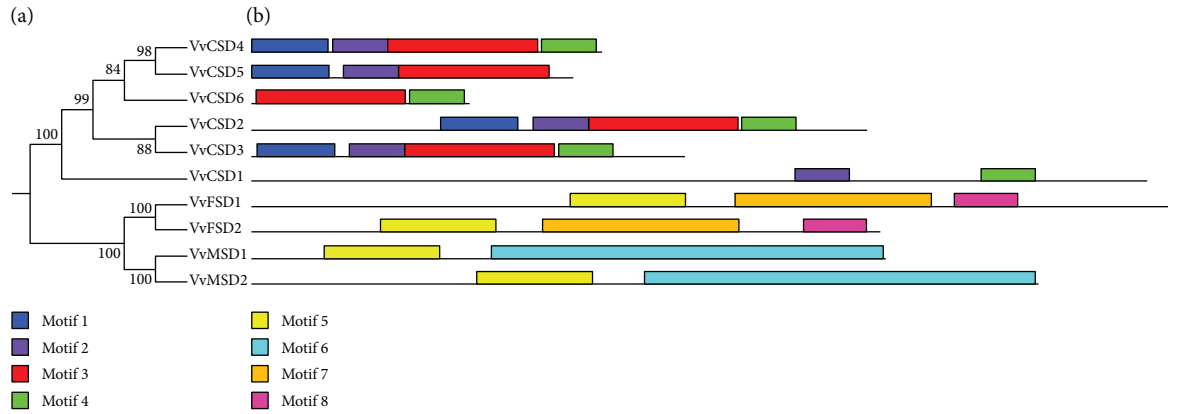

Figure 1: Unrooted neighbor-joining phylogenetic tree and conserved motif analysis of VvSOD proteins. (a) The phylogenetic tree was generated based on the protein sequences of VvSOD proteins. (b) Conserved motif analysis of VvSOD proteins. Different color boxes represent different types of motifs.

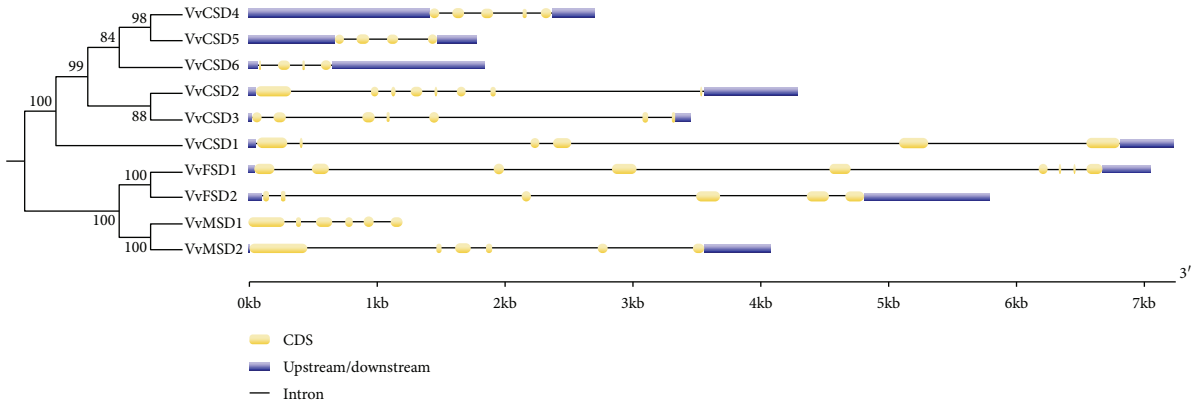

Figure 2: Gene structure of VvSOD genes. Blue boxes represent exons and lines represent introns.

(*VvCSD1*, *VvCSD2*, and *VvCSD5*) were positive, indicating that they are hydrophobic proteins and the rest of the VvSODs are hydrophilic proteins (Table 1).

The ProtComp9.0 program was used to predict the subcellular localizations of the VvSOD proteins. Among them, six Cu/ZnSODs were cytoplasmic, two MnSODs were in the mitochondria, and two FeSODs were located on the chloroplast (Table 1). These results were in accordance with a previous study [8, 37].

The MEME server was used for conserved motif analysis, and a total of eight conserved motifs were identified (Figure 1). Among them, motif 3 was observed in all six Cu/ZnSODs, while motifs 5, 6, and 7 were found in four Fe-MnSODs (Figure 2). The exon numbers varied among the 10 VvSODs, ranging from 4 to 9 (Figure 2). It is worth noting that the tandemly duplicated gene pair (*VvCSD4* and *VvCSD5*) and segmentally duplicated gene pair (*VvMSD1* and *VvMSD2*) both exhibited the same exon numbers.

3.2. Phylogenetic Analysis of SOD Genes. Twenty-eight SOD protein sequences from grapevine and *A. thaliana* (Table S1) were used to construct an unrooted phylogenetic tree (Figure 3). The SODs were divided into three major groups, namely, Cu/ZnSODs, MnSODs, and FeSODs. The FeSODs and MnSODs were clustered within a large clade with a high bootstrap value (99%), implying that the FeSODs and MnSODs originated from a common ancestor. Additionally, species-specific duplications occurred between *VvCSD4* and *VvCSD5* and *VvMSD1* and *VvMSD2*.

3.3. Chromosomal Locations and Syntenic Analysis. The 10 VvSOD genes were located on seven chromosomes, including *VvCSD1* on chromosome 2; *VvCSD2* and *VvMSD1* on chromosome 6; *VvCSD4*, *VvCSD5*, and *VvCSD6* on chromosome 14; and *VvCSD3*, *VvFSD1*, *VvMSD2*, and *VvFSD2* on chromosomes 8, 10, 13, and 16, respectively (Figure 4). One segmental duplication event was detected between gene *VvMSD1* and *VvMSD2* on chromosomes 6 and 13. Moreover, *VvCSD4* and *VvCSD5* were identified as a pair of tandemly duplicated genes. The Ka/Ks ratios were calculated to better understand the duplication and functional divergence of the duplicated VvSOD genes during their evolutionary course. As shown in Table S2, the Ka/Ks ratio of the segmentally duplicated gene pair (*VvMSD1* and *VvMSD2*) was 0.29, indicating that they underwent purifying selection. The Ka/Ks ratio of the tandemly

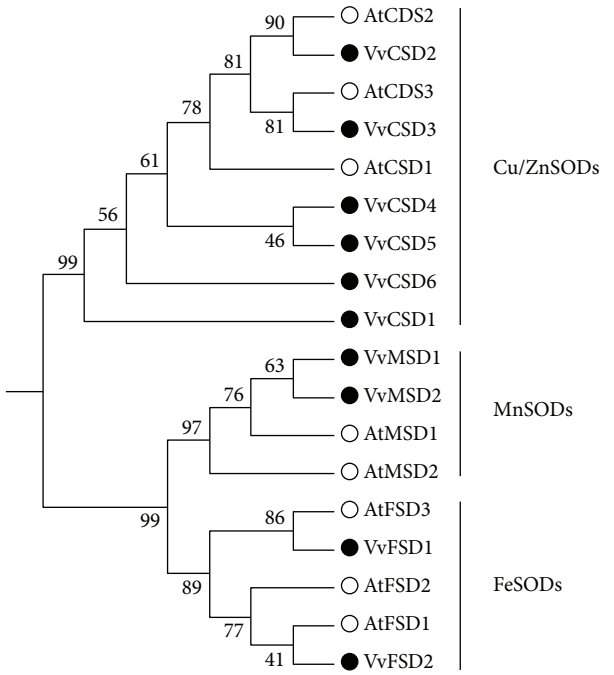

Figure 3: Phylogenetic tree of 77 SOD proteins from grape and other plants including *Arabidopsis thaliana*, *Oryza sativa*, *Sorghum bicolor*, *Populus trichocarpa*, *Amborella trichopoda*, *Cucumis sativus*, *Solanum lycopersicum*, and *Gossypium raimondii*. The Jones-Taylor-Thornton model with *P*-distance was chosen to conduct the phylogenetic tree. The bootstrap value was set as 1000. The SOD genes were classified into two major groups and five subfamilies (groups a, b, c, d, and e which have red, blue, yellow, purple, and green branches, respectively).

duplicated gene pair (*VvCSD4* and *VvCSD5*) was 1.29, which indicated that they were driven by positive selection during their evolutionary process.

3.4. GO Analysis of the VvSOD Proteins. Biological processes, molecular functions, and cellular components of genes are characteristics of genes or gene products that elucidate the diverse molecular functions of proteins [38]. GO analysis was performed to further characterize the predicted functions of the 10 VvSOD proteins (Figure 5). The "molecular function" data showed that all VvSOD genes were involved in the "superoxide dismutase activity" (GO:0004784). According to the "biological process" results, all of the VvSOD genes participated in the "oxidation-reduction process" (GO:0055114). Moreover, the grapevine SOD genes may be involved in the biological processes responding to biotic stimulus and abiotic stimulus, such as strong light, ozone, salt, and UV stresses. In addition, they may also participate in some biological metabolic processes, such as superoxide metabolic processes, tRNA metabolic processes, and rRNA processing.

3.5. Analysis of cis-Elements in Putative VvSOD Gene Promoters. To further determine the regulatory roles of VvSODs under various stresses, the *cis*-elements in the VvSOD gene promoter sequences were researched. The *cis*-elements were divided into four major subgroups: stress--responsive, hormone-responsive, light-responsive, and MYB binding site (Figure 6). Among 10 VvSODs, nine of them possessed several MYB binding sites. Furthermore, we found that abundant light-responsive *cis*-elements existed in the VvSODs, particularly in the *VvMSD2* gene with a number of 19.

3.6. Prediction of Potential Regulatory Interactions between TFs and VvSODs. To investigate the potential regulatory interactions between TFs and VvSODs, regulation prediction was done. A total of 21 TFs which possess overrepresented targets in the input gene set under a cutoff p value ≤ 0.05 were found. Among them, 10, 2, 9, 10, 9, 5, 1, 13, 3, and 8 TFs targeted *VvCSD1*, *VvCSD2*, *VvCSD3*, *VvCSD4*, *VvCSD5*, *VvCSD6*, *VvFSD1*, *VvFSD2*, *VvMSD1*, and *VvMSD2*, respectively (Table S6).

3.7. Expression Analysis of the VvSOD Genes Based on Microarray Data. To gain more insight into the role that VvSODs play in plant growth and development, we analyzed the expression patterns of the VvSOD genes in different grapevine tissues and organs based on the microarray data from 54 grapevine samples [33]. Interestingly, *VvMSD2* displayed consistently high expression in all 54 tissues, whereas *VvMSD1* exhibited lower expression levels compared with the others (Figure 7). *VvCSD4* and *VvCSD5* exhibited similar expression patterns in all the tested tissues. This similarity was also evident in gene *VvFSD1* and *VvFSD2*. Additionally, two genes (*VvMSD1* and *VvMSD2*) demonstrated distinct tissue-specific expression patterns.

Furthermore, four Affymetrix microarray datasets were specifically analyzed for determining the expression profiles of VvSODs and TF genes in response to abiotic stresses, which included PEG, salt, heat, and cold. Six out of 10 probes corresponding to VvSOD genes were found (*VvCSD1*, *VvCSD2*, *VvCSD3*, *VvCSD4*, *VvMSD2*, and *VvFSD1*). Eight out of 21 probes corresponding to TF genes were found (*VIT_18s0122g00380*, *VIT_17s0000g01260*, *VIT_08s0007g06270*, *VIT_04s0008g01470*, *VIT_05s0020g03880*, *VIT_19s0014g01680*, *VIT_15s0048g02870*, and *VIT_10s0003g00140*). In the cold, salt, and PEG stress, the expression levels of *VvCSD1* and *VvCSD2* were higher than those of the other four genes (Figure 8(a)). *VvFSD1* was expressed at an extremely low level in these three treatments. However, *VvCSD3* and *VvFSD1* were highly induced under the heat stress treatment. In each abiotic stress, there existed a single TF gene which responded strongly. However, the other was expressed at the similar level (Figure 8(b)). For example, listed genes, *VIT_10s0003g00140* in cold stress, *VIT_15s0048g02870* in salt and PEG stress, and *VIT_08s0007g06270* in heat stress, were all altered strongly by 8 times compared with the control. *VIT_10s0003g00140*, *VIT_15s0048g02870* and *VIT_08s0007g06270* belong to ERF, HD-ZIP, and SBP TF family, respectively (Table S6).

3.8. Expression Analysis of VvSOD Genes Based on qRT-PCR. Previous studies have demonstrated the important roles that SOD genes play in the plant response to abiotic stresses. The

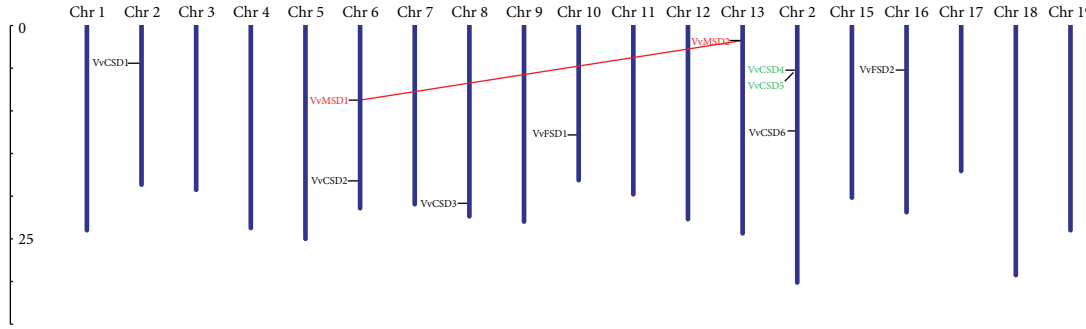

FIGURE 4: Chromosomal locations of 10 VvSOD genes on grape chromosomes. The chromosome numbers are indicated at the top of chromosomes, and the size of chromosomes is represented with a vertical scale. Segmental duplication relationships and DNA-based transposed duplication relationships among SOD genes are indicated in red and green, respectively.

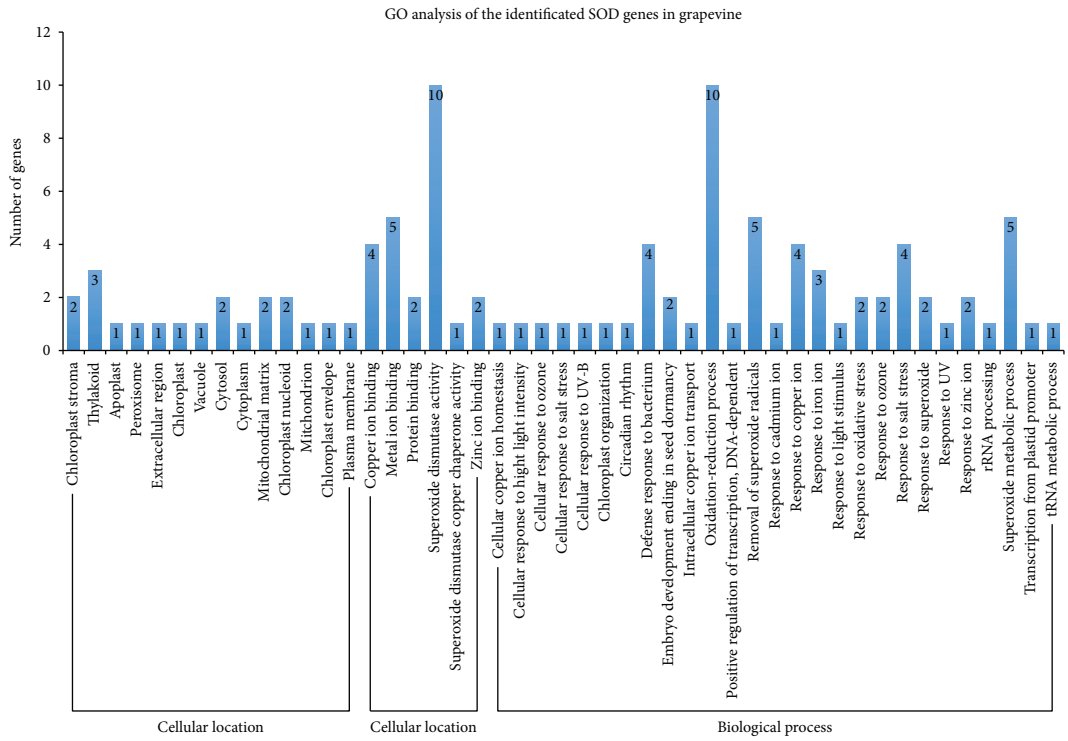

FIGURE 5: Gene ontology of SOD genes in grapevine. "Biological process," "cellular location," and "molecular function" were treated as independent attributes.

analysis of microarray data also indicated that the VvSOD genes were induced by different stresses. To gain more insight into the relative expressional diversity of eight members of the VvSOD gene family to cold, heat, salt, and drought, we detected the expression levels using qRT-PCR (Figure 9). Our results demonstrated that all eight VvSOD genes were induced noticeably by the four stresses, exhibiting different expression levels. All eight members were upregulated in the cold treatment, except for *VvCSD3* and *VvFSD2* (Figure 9). Among the six upregulated genes, *VvCSD1*, *VvCSD2*, and *VvFSD1* were altered strongly by 3–7.7 times compared with the control. Upon heat stress, expression of *VvCSD1* increased by 12-fold, 11-fold, and 9-fold at 6 h, 12 h, and 24 h, respectively. *VvCSD2*, *VvCSD3*, *VvFSD2*, and *VvMSD2* were also upregulated at 6 h with a lower expression level compared with that in *VvCSD1*. However, the other three genes (*VvCSD4*, *VvCSD6*, and *VvFSD1*) were downregulated during the treatment periods (Figure 9). In the salt treatment, the eight genes showed the lowest expression levels compared with the other three stresses. The expression levels of most of the genes exhibited slight variations, except *VvCSD3* and *VvCSD6*, which were upregulated more than 2-fold. Upon drought stress, the expression level of *VvCSD1*, *VvCSD2*, *VvCSD4*, and *VvCSD6* peaked at 12 h, but six genes (*VvCSD1*, *VvCSD2*, *VvCSD3*, *VvFSD1*, *VvFSD2*, and *VvMSD2*) were downregulated at 24 h. Only two genes (*VvCSD3* and *VvMSD2*) were downregulated at 6 h and maintained similar levels at the following time points.

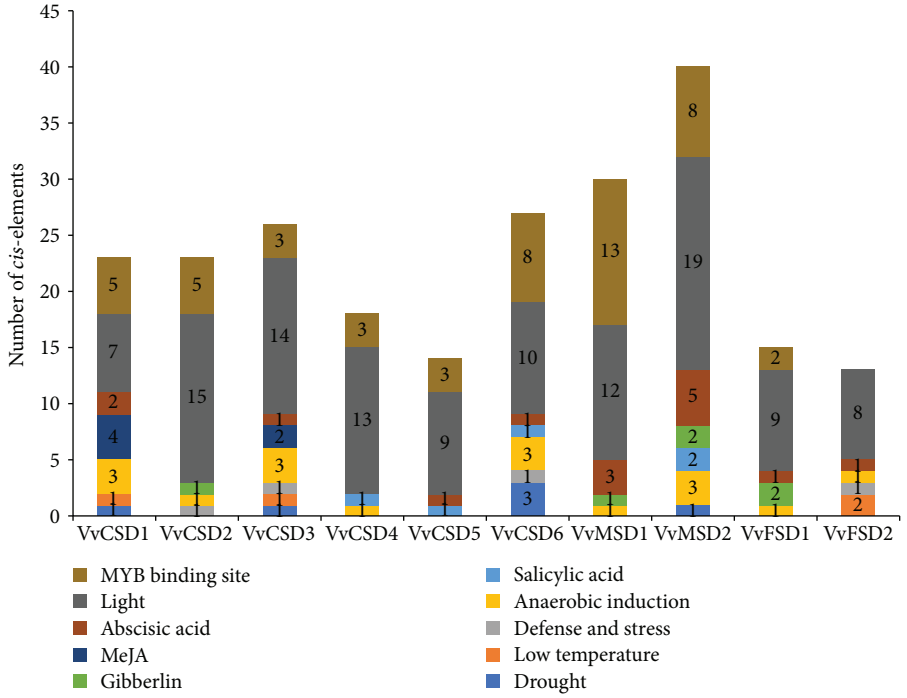

Figure 6: *cis*-element analysis of putative VvSOD promoters related to stress responses. Different *cis*-elements with the same or similar functions are shown in the same color.

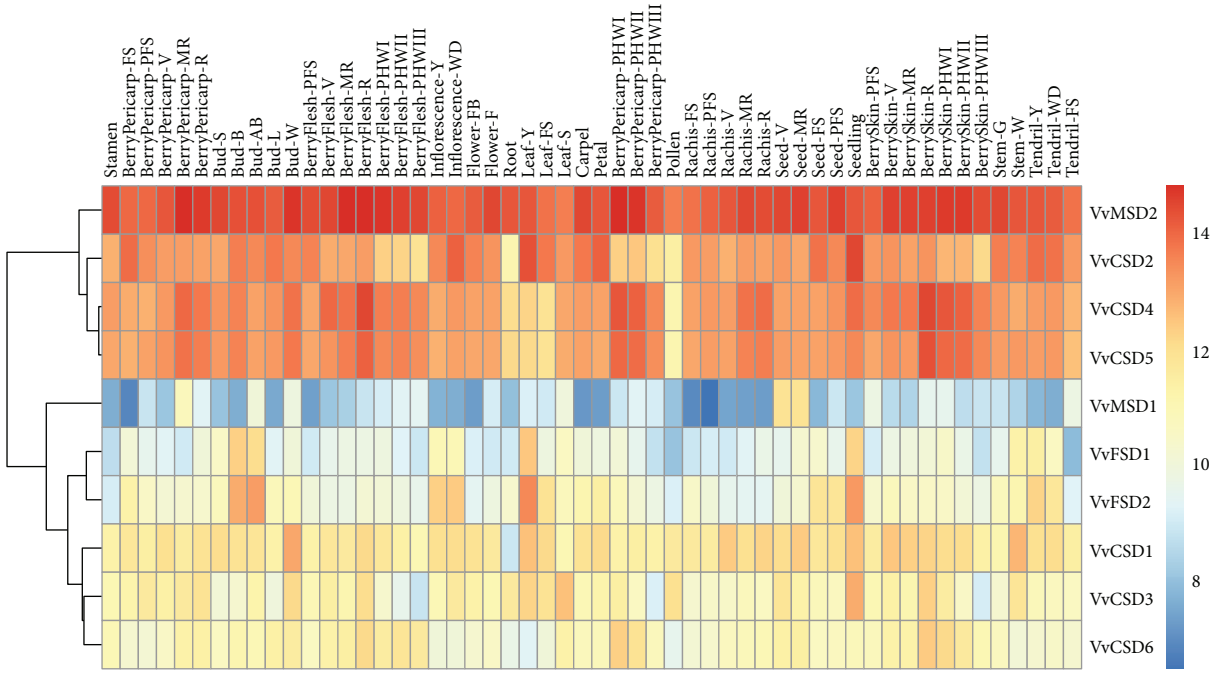

Figure 7: Expression profiles of 10 VvSODs in 54 different tissues and stages. Microarray data of the different organs of grapevine at various developmental stages were downloaded from Gene Expression Omnibus (GEO, available online: https://www.ncbi.nlm.nih.gov/geo/) under the accession number GSE36128, processing as log2 of the ratio and graphically represented with the RStudio software.

3.9. Coexpression Network of the VvSOD Gene Family and TF Genes. To determine the potential coexpression relationships between the VvSOD genes and TF genes, we conducted one coexpression network based on the microarray data under four stress treatments (p value < 0.05, and PCC<−0.95 or >0.95). It showed that VvSOD genes and TF genes corresponded both positively and negatively (Figure 10). A total of 11 gene pairs under three treatments (heat, salt,

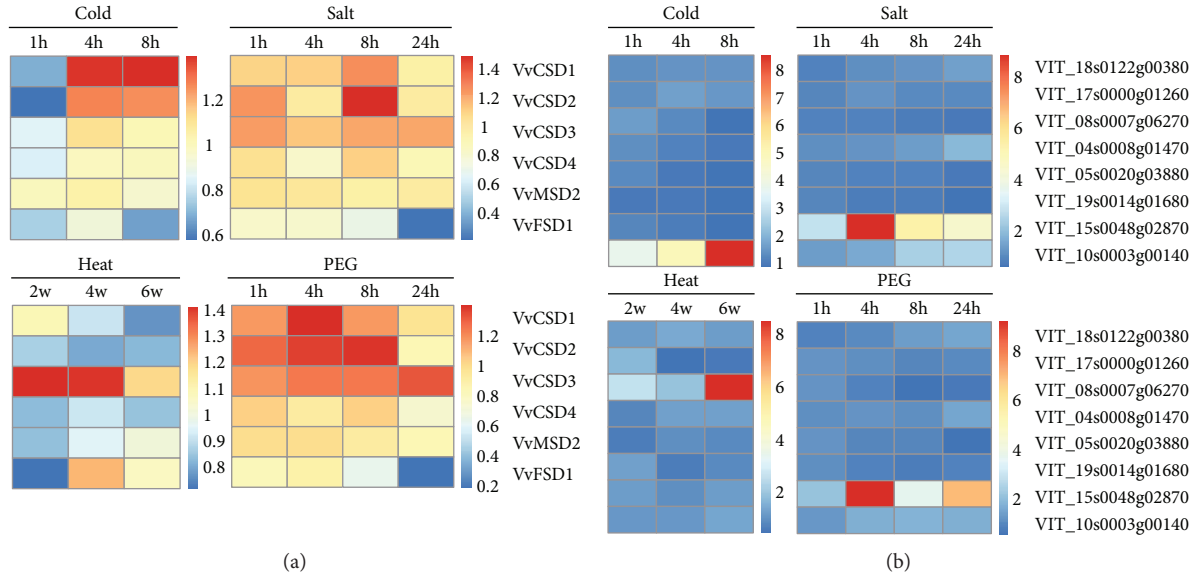

Figure 8: Expression profiles of the response of the grapevine VvSODs (a) and TF genes (b) to several abiotic stresses. Microarray data (accession number GSE31594 and GSE31675) downloaded from the NCBI GEO datasets. Four abiotic stresses, including salt, polyethylene glycol (PEG), heat, and cold, were analyzed. The fold changes compared with the corresponding control in each experiment were used to perform heatmaps that were generated by RStudio software.

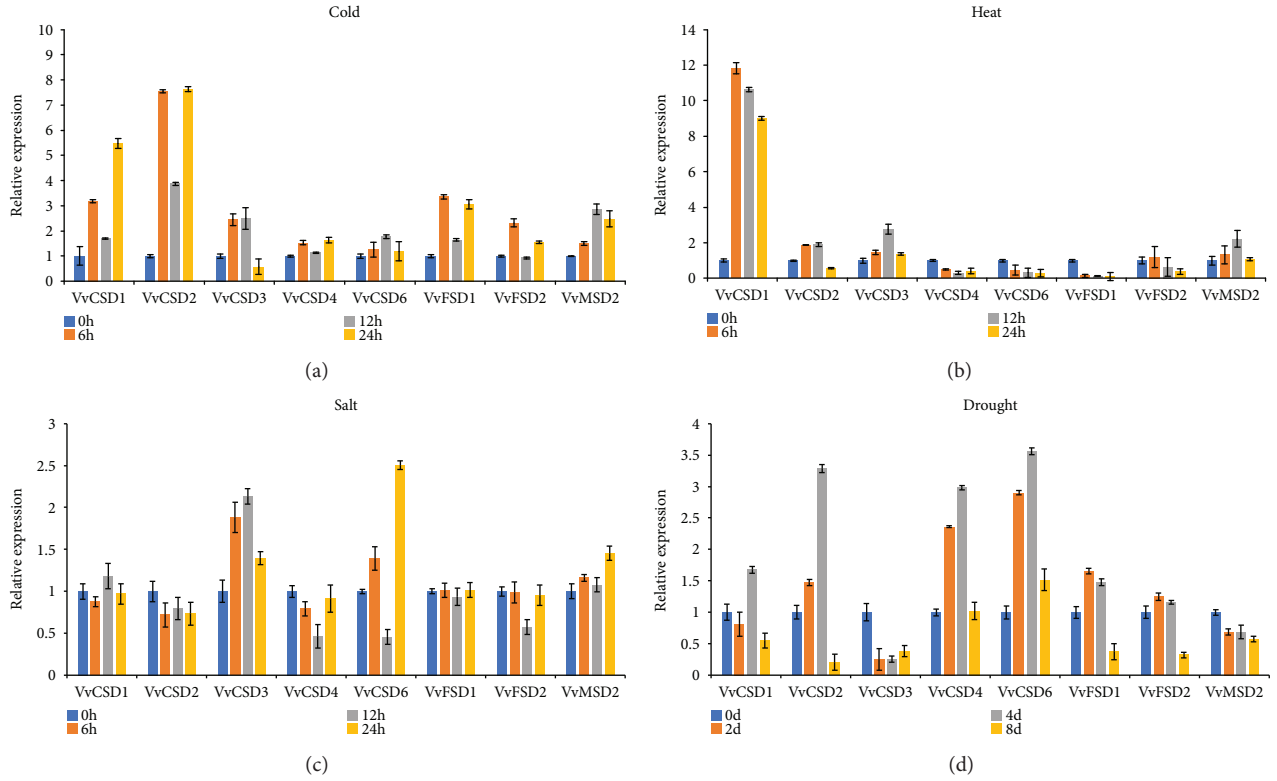

Figure 9: Quantitative real-time polymerase chain reaction (PCR) analysis of grape VvSODs in response to (a) cold stress, (b) heat stress, (c) salt stress (0 h, 6 h, 12 h, and 24 h), and (d) drought stress (0 days, 2 days, 4 days, and 8 days). Transcripts were normalized to the actin gene expression. The mean ± SD of the three biological replicates is presented.

and drought) were correlated with each other, including five VvSODs (*VvCSD2*, *VvCSD3*, *VvCSD4*, *VvMSD2*, and *VvFSD1*) and eight TF genes (*VIT_05s0020g03880*, *VIT_19s0014g01680*, *VIT_10s0003g00140*, *VIT_17s0000g01260*, *VIT_08s0007g06270*, *VIT_04s0008g01470*, *VIT_15s0048g02870*, *VIT_18s0122g00380*). Under heat treatment,

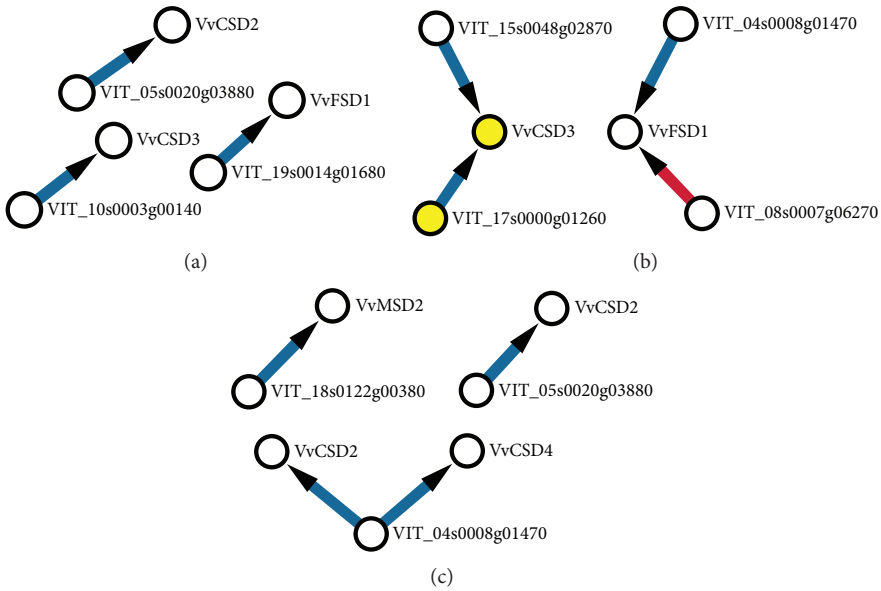

Figure 10: Coexpression networks of the grapevine SOD gene family and TF genes. The coexpression networks were established based on the Pearson correlation coefficients of gene pairs under cold, heat, drought, and salt stresses. All of the Pearson correlation coefficients of coexpression gene pairs were significant at the 0.05 significance level (p value). The different edge line colors indicated different relevance levels of coexpression gene pairs (the red color and blue color represent positive correlation and negative correlation, respectively). The arrow points from TF genes to VvSOD genes.

three gene pairs showed a negative correlation (Figure 10(a)). Only one gene pair was positively correlated with one another under salt stress (*VvFSD1* and *VIT_08s0007g06270*) (Figure 10(b)). Interestingly, correlated gene pair (*VvCSD3* and *VIT_17s0000g01260*, noted by yellow node) was also predicted to have regulation interaction (Table S6). Additionally, the result inferred that there was a negative correlation between *VIT_04s0008g01470* with two VvSOD genes (*VvCSD3* and *VvMSD2*) under PEG treatment (Figure 10(c)).

4. Discussion

With the development of second-generation sequencing technologies and the elucidation of the multiple functions of SOD genes, research into the identification of SOD genes has progressed rapidly. The SOD gene family has been identified in many species, such as *Arabidopsis* [20], longan [17], rice [39], poplar [9], banana [22], sorghum [40], tomato [8], cotton [23, 41], and cucumber [37].

In the present study, we identified 10 SOD genes in the grapevine genome that could be classified into three SOD types (six Cu/ZnSODs, two FeSODs, and two MnSODs) based on the domain and phylogenetic tree analyses. The 10 SOD genes possessed different intron numbers. A previous study reported that Cu/Zn-SODs containing different intron numbers and positions showed no exon-intron structural similarities in related species [42]. It is worth noting that one tandem pair of VvSOD genes (*VvMSD1* and *VvMSD2*) exhibited similar intron/exon organization patterns.

The promoters of VvSODs contain large amounts of light-responsive *cis*-elements that may contribute to light stress resistance. Gupta et al. detected increased resistance to oxidative stress in transgenic plants with an overexpressed Cu/Zn-SOD gene [43]. Transgenic *A. thaliana* plants overexpressing a miR398-resistant form of CSD2 accumulated more CSD2 mRNA than plants overexpressing a regular CSD2 and as a result were much more tolerant of intensive light [44]. Similar observations have also been reported in *Nicotiana tabacum* and *N. plumbaginifolia* [45, 46]. All VvSOD genes except for VvFSD2 possessed the MYB binding site. It had been reported that MYB transcription factors played regulatory roles in developmental processes and defense responses in plants [47]. The existence of abundant MYB-related *cis*-elements indicated that it may involve in the regulation of the expression of VvSOD genes.

By predicting TFs which may regulate VvSODs, several TFs were obtained (Table S6). These TFs belonged to a different TF protein family, including SBP, MYB, WRKY, ERF, CPP, LBD, TCP, HD-ZIP, AP2, and Dof family. Many of them had been found involve in a variety of biological functions like flower development, biotic and abiotic stresses, cell proliferation, hormonal response, and carbohydrate metabolism [48–54]. It has been reported that TFs regulate the target genes by both activate way and repress way [55, 56]. The coexpression results of VvSODs and TF genes also showed evidence for this conclusion. TF regulation prediction showed that *VIT_17s0000g01260* may interact with *VvCSD3*. Coexpression result identified this prediction with a negative relationship. However, the roles of TFs in VvSOD regulatory networks, as well as their interaction mechanism, remain to be fully elucidated through experimental verification and bioinformatic analysis.

Gene duplication provides new genetic material and novel genes and occurs via tandem, segmental, or genome-wide duplication [57–60]. In our study, only one segmental

duplication event (*VvMSD1* and *VvMSD2*) and one tandem duplication event (*VvCSD4* and *VvCSD5*) were identified.

The expression profiles of the 10 VvSOD genes in the different tissues indicated that most of the VvSOD genes were expressed, and a few genes displayed tissue-specific expression patterns. *VvCSD4* and *VvCSD5*, identified as tandemly duplicated gene pairs, exhibited similar gene expression patterns. Moreover, *VvMSD1* and *VvMSD2*, the segmentally duplicated gene pair, showed different expression patterns in all the tested tissues. Li et al. reported that the attribution of duplication mode to the expression divergence implies a different evolutionary course of duplicated genes [61]. Adams et al. found that organ-specific and biased expression or silencing of duplicated gene pairs existed in *Gossypium hirsutum* [62]. A similar phenomenon was also reported in wheat [63].

The qRT-PCR results revealed that every VvSOD gene responded to at least one abiotic stress treatment performed in our study (Figure 9). Notably, only *VvCSD1* was activated strongly under heat stress. Moreover, *VvCSD1* also expressed highly under cold stress. This suggest that *VvCSD1* may play a vital role in the low/high temperature defense. *VvCSD6* showed the highest expression level compared with other genes under drought stress. Promoter analysis revealed that *VvCSD6* harbored 3 MYB binding sites which involved in drought inducibility, which could explain the significant expression of *VvCSD6* under drought stress. Under salt stress, only the genes *VvCSD3* and *VvCSD6* altered obviously. Taken together, the expression pattern under various stress conditions suggested different VvSOD genes could perform its own function under different stresses. This research constitutes the first comprehensive study of the SOD gene family in grapevine and may provide valuable information for elucidating the classification, evolution, and putative functions of the grapevine SOD family on the whole-genome scale.

5. Conclusion

In the present study, we identified 10 SOD gene grapevine, including three types (6 Cu/Zn SODs, 2 FeSODs, and 2 MnSODs), which were unevenly distributed on 12 chromosomes. Syntenic analysis revealed that *VvMSD1* and *VvMSD2* were derived from segmental duplication, and *VvCSD4* and *VvCSD5* belong to a pair of tandemly duplicated genes. Promoter analysis indicated that VvSODs contain large amounts of light-responsive *cis*-elements which may contribute to light stress resistance. Furthermore, the expression profiles of the 10 VvSOD genes in the different tissues and abiotic stresses indicate that a few genes displayed tissue-specific expression patterns and VvSODs play roles in different aspects of abiotic stress. Finally, coexpression networks of VvSODs and TF genes under the four abiotic stresses were generated based on the microarray data. *VIT_17s0000g01260* predicted to regulate *VvCSD3*, coexpression analysis verified the corelationship of these two genes. This suggested that *VIT_17s0000g01260* may participate in the regulation of *VvCSD3*. However, the regulation mechanism needs further investigation.

This was the first comprehensive study of the SOD gene family in grapevine and may provide valuable information for understanding the classification, evolution, and putative functions of the grapevine SOD family on the genome-wide scale.

Data Availability

Previously reported microarray data were used to support this study and are available at the GEO dataset (https://www.ncbi.nlm.nih.gov/geo/). The accession numbers are in the following: GSE36128, GSE31594, and GSE31675. The qRT-PCR data used to support the findings of this study are included within the supplementary information file (Table S5).

Conflicts of Interest

The authors declare that there is no conflict of interest regarding the publication of this paper.

Acknowledgments

This work was partially supported by the Jiangsu Agriculture Science and Technology Innovation Fund (CX(16)1005), the National Natural Science Foundation of China (31501737), the open funds of the State Key Laboratory of Crop Genetics and Germplasm Enhancement (ZW201711), and the Fundamental Research Funds for the Central Universities (KJQN201655).

Supplementary Materials

Supplementary 1. Table S1: the grape and Arabidopsis SOD sequence information (including the name of each sequence, SOD type, and subcellular location) which is used for phylogenetic tree analysis.

Supplementary 2. Table S2: the Ka/Ks ratios for VvSOD proteins which were calculated using MEGA 6.06.

Supplementary 3. Table S3: the specific primer for qRT-PCR of each VvSOD gene.

Supplementary 4. Table S4: the Pearson correlation coefficient (PCC) value of four treatments. Coexpressed gene pairs were filtered with a PCC cutoff of 0.95.

Supplementary 5. Table S5: the PCR raw data of four treatments.

Supplementary 6. Table S6: basic information of the 21 TF genes.

References

[1] Y. Ma, J. Wang, Y. Zhong, F. Geng, G. R. Cramer, and Z. M. Cheng, "Subfunctionalization of cation/proton antiporter 1 genes in grapevine in response to salt stress in different organs," *Horticulture Research*, vol. 2, no. 1, article 15031, 2015.

[2] M. Tu, X. Wang, Y. Zhu et al., "VlbZIP30 of grapevine functions in dehydration tolerance via the abscisic acid core signaling pathway," *Horticulture Research*, vol. 5, no. 1, p. 49, 2018.

[3] J. P. Londo, A. P. Kovaleski, and J. A. Lillis, "Divergence in the transcriptional landscape between low temperature and freeze shock in cultivated grapevine (Vitis vinifera)," *Horticulture Research*, vol. 5, no. 1, 2018.

[4] T. Karuppanapandian, H. W. Wang, N. Prabakaran et al., "2,4-dichlorophenoxyacetic acid-induced leaf senescence in mung bean (Vigna radiata L. Wilczek) and senescence inhibition by co-treatment with silver nanoparticles," *Plant Physiology and Biochemistry*, vol. 49, no. 2, pp. 168–177, 2011.

[5] S. H. Lee, N. Ahsan, K. W. Lee et al., "Simultaneous overexpression of both CuZn superoxide dismutase and ascorbate peroxidase in transgenic tall fescue plants confers increased tolerance to a wide range of abiotic stresses," *Journal of Plant Physiology*, vol. 164, no. 12, pp. 1626–1638, 2007.

[6] J. M. Tepperman and P. Dunsmuir, "Transformed plants with elevated levels of chloroplastic SOD are not more resistant to superoxide toxicity," *Plant Molecular Biology*, vol. 14, no. 4, pp. 501–511, 1990.

[7] R. G. Alscher, N. Erturk, and L. S. Heath, "Role of superoxide dismutases (SODs) in controlling oxidative stress in plants," *Journal of Experimental Botany*, vol. 53, no. 372, pp. 1331–1341, 2002.

[8] K. Feng, J. Yu, Y. Cheng et al., "The SOD gene family in tomato: identification, phylogenetic relationships, and expression patterns," *Frontiers in Plant Science*, vol. 7, 2016.

[9] J. J. Molina-Rueda, C. J. Tsai, and E. G. Kirby, "The Populus superoxide dismutase gene family and its responses to drought stress in transgenic poplar overexpressing a pine cytosolic glutamine synthetase (GS1a)," *PLoS One*, vol. 8, no. 2, article e56421, 2013.

[10] J. J. P. Perry, D. S. Shin, E. D. Getzoff, and J. A. Tainer, "The structural biochemistry of the superoxide dismutases," *Biochimica et Biophysica Acta (BBA) - Proteins and Proteomics*, vol. 1804, no. 2, pp. 245–262, 2010.

[11] W. Wang, M. X. Xia, J. Chen, R. Yuan, F. N. Deng, and F. F. Shen, "Gene expression characteristics and regulation mechanisms of superoxide dismutase and its physiological roles in plants under stress," *Biochemistry*, vol. 81, no. 5, pp. 465–480, 2016.

[12] H.-D. Youn, E.-J. Kim, J.-H. Roe, Y. C. Hah, and S.-O. Kang, "A novel nickel-containing superoxide dismutase from Streptomyces spp," *Biochemical Journal*, vol. 318, no. 3, pp. 889–896, 1996.

[13] F. Wolfe-Simon, D. Grzebyk, O. Schofield, and P. G. Falkowski, "The role and evolution of superoxide dismutases in algae1," *Journal of Phycology*, vol. 41, no. 3, pp. 453–465, 2005.

[14] B. Wang, U. Lüttge, and R. Ratajczak, "Specific regulation of SOD isoforms by NaCl and osmotic stress in leaves of the C3 halophyte Suaeda salsa L," *Journal of Plant Physiology*, vol. 161, no. 3, pp. 285–293, 2004.

[15] M. Pilon, K. Ravet, and W. Tapken, "The biogenesis and physiological function of chloroplast superoxide dismutases," *Biochimica et Biophysica Acta-Bioenergetics*, vol. 1807, no. 8, pp. 989–998, 2011.

[16] A. C. Asensio, M. Gil-Monreal, L. Pires, Y. Gogorcena, P. M. Aparicio-Tejo, and J. F. Moran, "Two Fe-superoxide dismutase families respond differently to stress and senescence in legumes," *Journal of Plant Physiology*, vol. 169, no. 13, pp. 1253–1260, 2012.

[17] Y. L. Lin and Z. X. Lai, "Superoxide dismutase multigene family in longan somatic embryos: a comparison of CuZn-SOD, Fe-SOD, and Mn-SOD gene structure, splicing, phylogeny, and expression," *Molecular Breeding*, vol. 32, no. 3, pp. 595–615, 2013.

[18] D. Zhu and J. G. Scandalios, "Maize mitochondrial manganese superoxide dismutases are encoded by a differentially expressed multigene family," *Proceedings of the National Academy of Sciences*, vol. 90, no. 20, pp. 9310–9314, 1993.

[19] K. H. Baek, D. Z. Skinner, P. Ling, and X. Chen, "Molecular structure and organization of the wheat genomic manganese superoxide dismutase gene," *Genome*, vol. 49, no. 3, pp. 209–218, 2006.

[20] D. J. Kliebenstein, R. A. Monde, and R. L. Last, "Superoxide dismutase in Arabidopsis: an eclectic enzyme family with disparate regulation and protein localization," *Plant Physiology*, vol. 118, no. 2, pp. 637–650, 1998.

[21] E. Filiz and H. Tombuloğlu, "Genome-wide distribution of superoxide dismutase (SOD) gene families in Sorghum bicolor," *Turkish Journal of Biology*, vol. 39, no. 1, pp. 49–59, 2015.

[22] X. Feng, Z. Lai, Y. Lin, G. Lai, and C. Lian, "Genome-wide identification and characterization of the superoxide dismutase gene family in Musa acuminata cv. Tianbaojiao (AAA group)," *BMC Genomics*, vol. 16, no. 1, p. 823, 2015.

[23] W. Wang, M. Xia, J. Chen et al., "Genome-wide analysis of superoxide dismutase gene family in Gossypium raimondii and G. arboreum," *Plant Gene*, vol. 6, no. C, pp. 18–29, 2016.

[24] W. Wang, X. Zhang, F. Deng, R. Yuan, and F. Shen, "Genome-wide characterization and expression analyses of superoxide dismutase (SOD) genes in Gossypium hirsutum," *BMC Genomics*, vol. 18, no. 1, p. 376, 2017.

[25] E. Gasteiger, A. Gattiker, C. Hoogland, I. Ivanyi, R. D. Appel, and A. Bairoch, "ExPASy: the proteomics server for in-depth protein knowledge and analysis," *Nucleic Acids Research*, vol. 31, no. 13, pp. 3784–3788, 2003.

[26] T. L. Bailey, J. Johnson, C. E. Grant, and W. S. Noble, *Nucleic Acids Research*, vol. 43, no. W1, pp. W39–W49, 2015.

[27] K. Tamura, G. Stecher, D. Peterson, A. Filipski, and S. Kumar, "MEGA6: Molecular Evolutionary Genetics Analysis version 6.0," *Molecular Biology and Evolution*, vol. 30, no. 12, pp. 2725–2729, 2013.

[28] Y. Xi, J. Liu, C. Dong, and Z. M. (. M.). Cheng, "The CBL and CIPK gene family in grapevine (Vitis vinifera): genome-wide analysis and expression profiles in response to various abiotic stresses," *Frontiers in Plant Science*, vol. 8, p. 978, 2017.

[29] Y. Zhong and Z. M. Cheng, "A unique RPW8-encoding class of genes that originated in early land plants and evolved through domain fission, fusion, and duplication," *Scientific Reports*, vol. 6, no. 1, article 32923, 2016.

[30] K. Zhu, F. Chen, J. Liu, X. Chen, T. Hewezi, and Z. M. Cheng, "Evolution of an intron-poor cluster of the CIPK gene family and expression in response to drought stress in soybean," *Scientific Reports*, vol. 6, no. 1, article 28225, 2016.

[31] M. Lescot, P. Déhais, G. Thijs et al., "PlantCARE, a database of plant cis-acting regulatory elements and a portal to tools for in silico analysis of promoter sequences," *Nucleic Acids Research*, vol. 30, no. 1, pp. 325–327, 2002.

[32] J. Jin, F. Tian, D. C. Yang et al., "PlantTFDB 4.0: toward a central hub for transcription factors and regulatory

interactions in plants," *Nucleic Acids Research*, vol. 45, no. D1, pp. D1040–D1045, 2017.

[33] M. Fasoli, S. Dal Santo, S. Zenoni et al., "The grapevine expression atlas reveals a deep transcriptome shift driving the entire plant into a maturation program," *Plant Cell*, vol. 24, no. 9, pp. 3489–3505, 2012.

[34] K. Zhu, X. Wang, J. Liu et al., "The grapevine kinome: annotation, classification and expression patterns in developmental processes and stress responses," *Horticulture Research*, vol. 5, no. 1, p. 19, 2018.

[35] M. Wang, A. Vannozzi, G. Wang et al., "Genome and transcriptome analysis of the grapevine (Vitis vinifera L.) WRKY gene family," *Horticulture Research*, vol. 1, no. 1, article 14016, 2014.

[36] J. Liu, N. Chen, F. Chen et al., "Genome-wide analysis and expression profile of the bZIP transcription factor gene family in grapevine (Vitis vinifera)," *BMC Genomics*, vol. 15, no. 1, p. 281, 2014.

[37] Y. Zhou, L. Hu, H. Wu, L. Jiang, and S. Liu, "Genome-wide identification and transcriptional expression analysis of cucumber superoxide dismutase (SOD) family in response to various abiotic stresses," *International Journal of Genomics*, vol. 2017, Article ID 7243973, 14 pages, 2017.

[38] M. Ashburner, C. A. Ball, J. A. Blake et al., "Gene ontology: tool for the unification of biology. The gene ontology consortium," *Nature Genetics*, vol. 25, no. 1, pp. 25–29, 2000.

[39] B. Dehury, K. Sarma, R. Sarmah et al., "In silico analyses of superoxide dismutases (SODs) of rice (Oryza sativa L.)," *Journal of Plant Biochemistry and Biotechnology*, vol. 22, no. 1, pp. 150–156, 2013.

[40] E. Filiz and H. Tombuloğlu, "Genome-wide distribution of superoxide dismutase (SOD) gene families inSorghum bicolor," *Turkish Journal of Biology*, vol. 39, pp. 49–59, 2015.

[41] J. Zhang, B. Li, Y. Yang et al., "Genome-wide characterization and expression profiles of the superoxide dismutase gene family in Gossypium," *International Journal of Genomics*, vol. 2016, Article ID 8740901, 11 pages, 2016.

[42] R. C. Fink and J. G. Scandalios, "Molecular evolution and structure–function relationships of the superoxide dismutase gene families in angiosperms and their relationship to other eukaryotic and prokaryotic superoxide dismutases," *Archives of Biochemistry and Biophysics*, vol. 399, no. 1, pp. 19–36, 2002.

[43] A. S. Gupta, J. L. Heinen, A. S. Holaday, J. J. Burke, and R. D. Allen, "Increased resistance to oxidative stress in transgenic plants that overexpress chloroplastic Cu/Zn superoxide dismutase," *Proceedings of the National Academy of Sciences*, vol. 90, no. 4, pp. 1629–1633, 1993.

[44] R. Sunkar, A. Kapoor, and J. K. Zhu, "Posttranscriptional induction of two Cu/Zn superoxide dismutase genes in Arabidopsis is mediated by downregulation of miR398 and important for oxidative stress tolerance," *Plant Cell*, vol. 18, no. 8, pp. 2051–2065, 2006.

[45] J. Kurepa, M. V. Montagu, and D. Inzé, "Expression of sodCp and sodB genes in Nicotiana tabacum: effects of light and copper excess," *Journal of Experimental Botany*, vol. 48, no. 12, pp. 2007–2014, 1997.

[46] E. W. Tsang, C. Bowler, D. Hérouart et al., "Differential regulation of superoxide dismutases in plants exposed to environmental stress," *Plant Cell*, vol. 3, no. 8, pp. 783–792, 1991.

[47] C. Yanhui, Y. Xiaoyuan, H. Kun et al., "The MYB transcription factor superfamily of Arabidopsis: expression analysis and phylogenetic comparison with the rice MYB family," *Plant Molecular Biology*, vol. 60, no. 1, pp. 107–124, 2006.

[48] K. Yamasaki, T. Kigawa, M. Inoue et al., "A novel zinc-binding motif revealed by solution structures of DNA-binding domains of Arabidopsis SBP-family transcription factors," *Journal of Molecular Biology*, vol. 337, no. 1, pp. 49–63, 2004.

[49] S. P. Pandey and I. E. Somssich, "The role of WRKY transcription factors in plant immunity," *Plant Physiology*, vol. 150, no. 4, pp. 1648–1655, 2009.

[50] M. Martín-Trillo and P. Cubas, "TCP genes: a family snapshot ten years later," *Trends in Plant Science*, vol. 15, no. 1, pp. 31–39, 2010.

[51] T. Nakano, K. Suzuki, T. Fujimura, and H. Shinshi, "Genome--wide analysis of the ERF gene family in Arabidopsis and rice," *Plant Physiology*, vol. 140, no. 2, pp. 411–432, 2006.

[52] D. Lijavetzky, P. Carbonero, and J. Vicente-Carbajosa, "Genome-wide comparative phylogenetic analysis of the rice and Arabidopsis Dof gene families," *BMC Evolutionary Biology*, vol. 3, no. 1, p. 17, 2003.

[53] Z. Yang, S. Gu, X. Wang, W. Li, Z. Tang, and C. Xu, "Molecular evolution of the CPP-like gene family in plants: insights from comparative genomics of Arabidopsis and rice," *Journal of Molecular Evolution*, vol. 67, no. 3, pp. 266–277, 2008.

[54] R. Stracke, M. Werber, and B. Weisshaar, "The R2R3-MYB gene family in Arabidopsis thaliana," *Current Opinion in Plant Biology*, vol. 4, no. 5, pp. 447–456, 2001.

[55] T. Eulgem, P. J. Rushton, S. Robatzek, and I. E. Somssich, "The WRKY superfamily of plant transcription factors," *Trends in Plant Science*, vol. 5, no. 5, pp. 199–206, 2000.

[56] D. S. Latchman, "Transcription factors: bound to activate or repress," *Trends in Biochemical Sciences*, vol. 26, no. 4, pp. 211–213, 2001.

[57] A. R. Kersting, E. Bornberg-Bauer, A. D. Moore, and S. Grath, "Dynamics and adaptive benefits of protein domain emergence and arrangements during plant genome evolution," *Genome Biology and Evolution*, vol. 4, no. 3, pp. 316–329, 2012.

[58] M. Buljan and A. Bateman, "The evolution of protein domain families," *Biochemical Society Transactions*, vol. 37, no. 4, pp. 751–755, 2009.

[59] X. Yang, G. A. Tuskan, and Z.-M. Cheng, "Divergence of the Dof gene families in poplar, Arabidopsis, and rice suggests multiple modes of gene evolution after duplication," *Plant Physiology*, vol. 142, no. 3, pp. 820–830, 2006.

[60] Y. Zhong, Y. Jia, Y. Gao, D. Tian, S. Yang, and X. Zhang, "Functional requirements driving the gene duplication in 12 Drosophila species," *BMC Genomics*, vol. 14, no. 1, p. 555, 2013.

[61] Z. Li, H. Zhang, S. Ge, X. Gu, G. Gao, and J. Luo, "Expression pattern divergence of duplicated genes in rice," *BMC Bioinformatics*, vol. 10, no. S6, p. S8, 2009.

[62] K. L. Adams, R. Cronn, R. Percifield, and J. F. Wendel, "Genes duplicated by polyploidy show unequal contributions to the transcriptome and organ-specific reciprocal silencing," *Proceedings of the National Academy of Sciences*, vol. 100, no. 8, pp. 4649–4654, 2003.

[63] A. Bottley, G. M. Xia, and R. M. D. Koebner, "Homoeologous gene silencing in hexaploid wheat," *The Plant Journal*, vol. 47, no. 6, pp. 897–906, 2006.